Automatica 49 (2013) 285–292

Contents lists available at SciVerse ScienceDirect

Automatica

journal homepage: www.elsevier.com/locate/automatica

Brief paper

A bounded controller for multirobot navigation while maintaining network connectivity in the presence of obstacles☆

Xiangpeng Li [a], Dong Sun [a,1], Jie Yang [b]

[a] Department of Mechanical and Biomedical Engineering, City University of Hong Kong, Hong Kong, China

[b] Department of Precision Machinery and Precision Instrumentations, University of Science and Technology of China, China

ARTICLE INFO

Article history:
Received 27 November 2011
Received in revised form
31 July 2012
Accepted 25 August 2012
Available online 26 November 2012

Keywords:
Multirobot control
Network connectivity
Obstacle avoidance
Navigation

ABSTRACT

Maintaining the connectivity of networked robots is a challenge in multirobot applications. In this paper, this challenging problem is addressed through the development of a novel controller that can guarantee that robots will approach their individual desired positions while maintaining existing network topology and avoiding obstacles. A new concept of connectivity constraint, along with a continuous modeling approach to obstacle avoidance, is utilized in building the navigation function. The designed potential field integrates the navigation requirement, connectivity constraint, and obstacle avoidance simultaneously, based on which a bounded control input is generated for multirobot control. It is shown that if the initial configurations of the robots are connected and the desired configuration is reachable, the proposed controller is capable of driving multirobots to their individual goal positions conditionally while keeping the underlying network connected. Simulations and experiments are finally performed using a group of mobile robots to demonstrate the effectiveness of the proposed controller.

1. Introduction

Cooperative control of multirobots has recently received considerable attention as regards solving such problems as network consensus (Ji & Egerstedt, 2007; Ren & Beard, 2005; Saber & Murray, 2004; Wang & Guo, 2008), formation (Chen, Sun, Yang, & Chen, 2010a,b; Guo & Qu, 2008; Lu & Guo, 2010; Sun, Wang, Shang, & Feng, 2009; Tanner, Jadbabaie, & Pappas, 2007; Yan, Chen, & Sun, 2012; Zheng & Chen, 2007), coverage problems (Cortes, Martinez, Karatas, & Bullo, 2004; Guo & Balakrishnan, 2006), region-reaching control (Cheah, Hou, & Slotine, 2009; Cheah, Wang, & Sun, 2007), and multirobot navigation (Liu, Sun, & Zhu, 2011; Loizou & Kyriakopoulos, 2006; Lumelsky & Harinarayan, 1997). In most of these applications, the robots are assumed to remain entirely connected to one another for information exchange. In practice, however, guaranteeing that the robots would maintain connectivity in multirobot tasks is difficult, given that robot motions may split communication links easily.

Maintaining connectivity among robots is important for numerous multirobot navigation applications. In the coverage control of mobile sensing networks (Cortes et al., 2004; Cortes, Martinez, Karatas, & Bullo, 2005), the centroid of the corresponding Voronoi cell was dynamically shared as the desired position for all the robots, such that the robots moved to their desired positions while maintaining connectivity. In the mobile router task (Tekdas, Kumar, Isler, & Janardan, 2012), every "bridge node" robot moved to its desired position while maintaining the communication link between the "user" and the "station". In exploration and mapping tasks (Sheng, Yang, Tan, & Xi, 2006), environmental information was shared amongst all the robots for all tasks. In these applications, the robots have access to their desired goals but still need to be connected with one another to accomplish the multirobot tasks.

The issue of network connectivity has been investigated particularly in terms of consensus, formation, and rendezvous. The main approaches found in the literature include the geometric constraint technique (Ando, Oasa, Suzuki, & Yamashita, 1999; Savla, Notarstefano, & Bullo, 2009; Spanos & Murray, 2004), algebraic graph theory-based approaches (DeGennaro & Jadbabaie, 2006; Kim & Mesbahi, 2005; Stump, Jadbabaie, & Kumar, 2008), and the artificial potential field method (Gazi & Passino, 2004; Ji & Egerstedt, 2007; Shi, Wang, & Chu, 2006; Tanner et al., 2007; Tardioli, Mosteo, Riazuelo, Villarroel, & Montano, 2010). In the study of Dimarogonas and Johansson (2008), a feedback controller was proposed for accomplishing the rendezvous task

☆ This work was supported by the Research Grants Council, Hong Kong Special Administrative Region, China, under Grant CityU 119612. The material in this paper was partially presented at the 2010 IEEE/RSJ International Conference on Intelligent Robots and Systems (IROS 2010), October 18–22, 2010, Taipei, Taiwan. This paper was recommended for publication in revised form by Associate Editor C.C. Cheah under the direction of Editor Toshiharu Sugie.

E-mail addresses: xiangpli@cityu.edu.hk (X. Li), medsun@cityu.edu.hk (D. Sun), jieyang@ustc.edu.cn (J. Yang).

[1] Tel.: +852 3442 8405; fax: +852 3442 0172.

0005-1098/$ – see front matter © 2012 Elsevier Ltd. All rights reserved.
doi:10.1016/j.automatica.2012.10.014

while maintaining robot network connectivity with bounded control inputs in an obstacle-free environment. Extending this work, the performance of a rendezvous task while maintaining network connectivity in the presence of obstacles was recently achieved (Li, Sun, & Yang, 2010).

This study proposes the use of the artificial potential field method to solve the connectivity problem in a multirobot navigation task. A new concept termed the connectivity constraint is first proposed in establishing the objective function for maintaining connectivity. Introducing the concept of a virtual obstacle, a continuous model is designed to formulate obstacle avoidance. The connectivity constraint and the continuous model for obstacle avoidance are then incorporated into the design of a multirobot navigation function, based on which a controller is designed as a negative gradient of this navigation function.

The proposed method exhibits three advantages. First, the current method employs a decentralized controller that can address multirobot navigation, network connectivity maintenance, and obstacle avoidance simultaneously. The existing multirobot navigation approaches, such as those by Liu et al. (2011) and Lumelsky and Harinarayan (1997), solved the multirobot navigation problem but did not consider the issue of connectivity maintenance. The relevant research by Ayanian and Kumar (2008) required that the information on the global environment and the state of each robot be known. Second, the current method employs a continuous model to solve the problem of obstacle avoidance for robots with limited sensing capabilities, thus allowing the application of the proposed navigation approach in unknown environments. Notably, the traditional navigation function-based approaches, such as those by Loizou and Kyriakopoulos (2006) and Rimon and Koditschek (1992), required global information on the environment and could only work well in a known environment. Third, the current method is designed on the basis of an analysis of the polar property of the proposed navigation function. Our study shows that if the initial configurations of the robots are connected and the desired configuration is reachable, the proposed controller can drive multirobots to their individual goal positions conditionally while maintaining the underlying network connected. Few existing approaches have achieved such a result.

2. Modeling

We consider n robots in a workspace $W \in \Re^2$. The position coordinate of the ith robot is denoted as $q_i(t) \in \Re^2$. The dynamics of the ith robot is represented as follows:

$$\dot{q}_i = u_i, \quad i \in \{1, \ldots, n\} \tag{1}$$

where $u_i \in \Re^2$ denotes the velocity control input of the ith robot. The position vector $\mathbf{q} = [q_1(t)^T, \ldots, q_n(t)^T]^T$ and the control input vector $\mathbf{u} = [u_1(t)^T, \ldots, u_n(t)^T]^T$ are introduced. The desired destinations of the robots are denoted as $\mathbf{q^d} = [(q_1^d)^T, \ldots, (q_i^d)^T, \ldots, (q_n^d)^T]^T$, where $q_i^d \in \Re^2$ is the desired destination of the ith robot.

Furthermore, we consider that there are m obstacles located in the workspace. The coordinate of the ςth obstacle is denoted by $q_o(\varsigma) \in \Re^2$, where $\varsigma \in \{1, \ldots, m\}$ is the index of obstacles. Similarly, positions of all obstacles can be represented by a vector $\mathbf{q}_0 = \left[q_o(1)^T, \ldots, q_o(m)^T\right]^T$. For simplicity, each robot was treated as a sphere.

2.1. Connectivity constraint

Given the limited sensing and communication capability, the ith robot can communicate with the other robots only when these robots are located within a reachable area, which is denoted by a circle with radius r and centered at $q_i(t)$. The communication topology is associated with the communication graph.

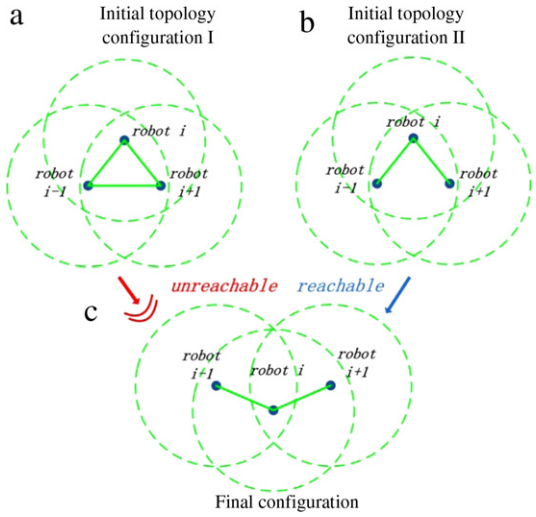

Fig. 1. Example of a reachable topology.

Definition 1 (*Communication Graph*)**.** The communication graph $I(t) = (V, E)$ is an undirected graph, which consists of a set of vertices $V = \{1, \ldots, n\}$ as indices of robots, as well as a set of edges $E \subset V \times V$ as indices of available communication links amongst the robots, where $E = \left\{(i, j) \mid d_{ij} < r\right\}$ consists of a pair of robots i and j, $d_{ij}(t) = \left\|q_i(t) - q_j(t)\right\|$ denotes the Euclidean distance between the ith and the jth robots, and r denotes the communication radius of the ith robot. We define $N(i) = \{j \mid (i, j) \in E\}$ as the set containing all neighboring robots of the ith robot.

This study focuses on the connectivity maintenance of an existing communication topology. The issue of the creation of new communication topology is not the focus of this paper. A number of available topology creation algorithms, such as those discussed in Tardioli et al. (2010) and Zavlanos, Tanner, Jadbabaie, and Pappas (2009), can be used in selecting the topology from the communication graph.

To confine the underlying relationship between the current communication topology of robots and the final configuration of robots, the concept of reachable topology must first be clarified. Fig. 1 illustrates a network with three robots, where each robot is denoted by a small disc. The solid line denotes the existing communication link between two robots, and the dotted circle denotes the communication range. The final configuration is illustrated in Fig. 1(c), showing that the distance between robot $i-1$ and robot $i+1$ is beyond the communication range of the robot. Thus, the final configuration cannot be reached by robots with the initial configuration shown in Fig. 1(a). However, if the link $(i-1, i+1)$ is deleted from the initial topology configuration, as shown in Fig. 1(b), the final configuration becomes reachable. The reachable topology is hence formulated as below.

Definition 2 (*Reachable Topology*)**.** The desired configuration $\mathbf{q^d}$ is reachable if the following condition holds:

$$\left\|q_i^d - q_j^d\right\| < r, \quad \forall i \in \{1, \ldots, n\}, j \in N(i). \tag{2}$$

In the following development, the constraint given in (2) will apply to all the desired robot destinations.

For the ith robot, we introduce the following connectivity constraint:

$$G_c(q_i(t)) = \prod_{j \in N(i)} \frac{1}{2}\left(r^2 - d_{ij}(t)^2\right) = \prod_{j \in N(i)} \beta_{ij}. \tag{3}$$

To maintain the connectivity between the ith robot and all its neighbors in $N(i)$, $G_c(q_i(t)) > 0$ must always hold true.

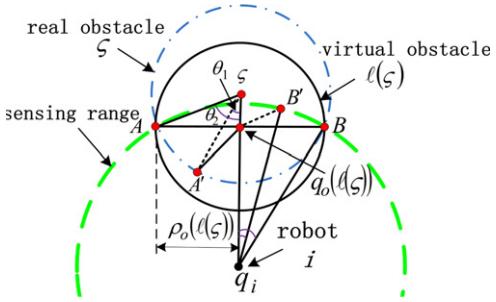

Fig. 2. Obstacle encountering process under the continuous model for obstacle avoidance.

2.2. Obstacle avoidance

To aid in the formulation of the problem of obstacle avoidance, a continuous model should be employed to smooth the obstacle encountering process. Saber (2006) proposed the use of a virtual agent located on the boundary of the obstacle to represent the real obstacle for avoidance. Motivated by this concept, we use a virtual obstacle denoted by $\ell(\varsigma)$ to simulate the encountered part of the obstacle ς, as shown in Fig. 2. Obstacle ς is represented by the circle with a chain line, and the virtual obstacle $\ell(\varsigma)$ is represented by the circle with a solid line. As previously mentioned, the obstacles in this paper are modeled as spheres. For the obstacle ς with irregular shapes, $\ell(\varsigma)$ can be represented as the circumcircle of the encountered part of ς, where line AB denotes the maximum breadth of $\ell(\varsigma)$, while q_A and q_B can be measured by the sonar or vision system equipped in the robot. The points A' and B' denote the two arbitrary points in inferior arcs $AA'B$ and $AB'B$. The sensing range of robot i is represented by the circle with a dotted line, and for simplicity, it is set to be the same as the communication range of the other robots.

Proposition 1. *When the obstacle ς is located inside (or partly inside) the sensing range of robot i, it can be simulated as a virtual sphere obstacle $\ell(\varsigma)$, located at $q_o(\ell(\varsigma))$ with a radius of $\rho_o(\ell(\varsigma))$. Thus, $q_o(\ell(\varsigma))$ and $\rho_o(\ell(\varsigma))$ can be calculated as follows:*

$$\begin{aligned}\rho_o(\ell(\varsigma)) &= \frac{1}{2}\|q_A - q_B\|,\\ q_o(\ell(\varsigma)) &= \frac{1}{2}(q_A + q_B).\end{aligned} \tag{4}$$

When the obstacle ς is located outside the sensing range of robot i, it is simulated as a virtual point obstacle $\ell(\varsigma)$, located at the boundary of the sensing range of robot i, with a radius of $\rho_o(\ell(\varsigma)) = 0$.

The proposed virtual obstacle $\ell(\varsigma)$ covers the encountered part of the real obstacle ς, which can be verified by showing that $\rho_o(\ell(\varsigma)) \geq \max\left\{d_{A'q_o(\ell(\varsigma))}, d_{B'q_o(\ell(\varsigma))}\right\}$. In triangles $\triangle A\varsigma q_o(\ell(\varsigma))$ and $\triangle A'\varsigma q_o(\ell(\varsigma))$, the following can be achieved:

$$\begin{aligned}d_{A'q_o(\ell(\varsigma))} &= \sqrt{\left(d_{A'\varsigma}\right)^2 + \left(d_{\varsigma q_o(\ell(\varsigma))}\right)^2 - 2d_{A'\varsigma}d_{\varsigma q_o(\ell(\varsigma))}\cos\theta_1}\\ &\leq \sqrt{\left(d_{A\varsigma}\right)^2 + \left(d_{\varsigma q_o(\ell(\varsigma))}\right)^2 - 2d_{A\varsigma}d_{\varsigma q_o(\ell(\varsigma))}\cos\theta_2}\\ &= d_{Aq_o(\ell(\varsigma))} = \rho_o(\ell(\varsigma)).\end{aligned} \tag{5}$$

Similarly, $d_{q_o(\ell(\varsigma))B'} \leq d_{q_o(\ell(\varsigma))B} = \rho_o(\ell(\varsigma))$ can be obtained in triangles $\triangle B'q_iq_o(\ell(\varsigma))$ and $\triangle Bq_iq_o(\ell(\varsigma))$.

A smooth constraint function $G_o(q_i(t))$ is introduced for obstacle avoidance, which is expressed as

$$G_o(q_i(t)) = \left(\frac{r^2}{2}\right)^{m-|O(i)|}\prod_{\ell(\varsigma)\in O(i)}\alpha_{i\ell(\varsigma)} \tag{6}$$

where $O(i)$ denotes a set of obstacles encountered by the ith robot, which is obtained on the basis of Proposition 1; $|O(i)|$ denotes the cardinality of set $O(i)$; and $\alpha_{i\ell(\varsigma)} = \frac{1}{2}\left(d^2_{i\ell(\varsigma)} - \rho_o^2(\ell(\varsigma))\right)$. In the follow-on development, the "obstacle" actually refers to "the virtual obstacle".

According to Proposition 1, the function $G_o(q_i(t))$ is always continuous. Therefore, the obstacle encountering process is continuous.

Unlike traditional approaches to avoiding obstacles (such as that of Stipanović, Hokayem, Spong, and Šiljak (2007)), where the information on the whole obstacle must be known, the proposed continuous algorithm only requires local information, that is, the encountered part of the obstacle, to be known in the obstacle encountering process.

In a similar way, the collision avoidance among the robots can be achieved as discussed in Li, Sun, Yang, and Liu (2011).

2.3. Free workspace

We now discuss the concept of free workspace. The free workspace F_i is defined as a subset of the robot position $q_i(t)$ that meets the connectivity constraint while avoiding obstacles.

Definition 3 (*Free Workspace, F_i*)**.**

$$F_i = \{q_i(t) \,|\, G(q_i(t)) = G_c(q_i(t))\, G_o(q_i(t)) > 0\}. \tag{7}$$

The above definition implies that in the free workspace, the robot can maintain connectivity with its neighbors $N(i)$ while avoiding obstacles in its sensing range. The connectivity control problem can, thus, be formulated as follows:

Problem 1 (*Connectivity Control*)**.** Considering n networked robots with initial configuration of $G(q_i(0)) > 0, \forall i \in \{1, \ldots, n\}$, we determine the bounded control input $\mathbf{u}$ such that $G(q_i(t)) > 0, \forall i \in \{1, \ldots, n\}$, can be obtained all the time.

3. Control design

In a manner similar to that of the work of Rimon and Koditschek (1992), a bounded navigation potential field $\varphi_i \in [0, 1]$ was designed, which is expressed as

$$\varphi_i = \frac{\gamma(q_i(t))}{\left(\gamma^\delta(q_i(t)) + G(q_i(t))\right)^{\frac{1}{\delta}}} \tag{8}$$

where δ is a positive parameter, and $\gamma(q_i)$ is expressed as

$$\gamma(q_i(t)) = \frac{1}{2}e_i^T e_i = \frac{1}{2}\left\|\nabla_{q_i}\gamma(q_i(t))\right\|^2 \tag{9}$$

where $e_i = q_i - q_i^d$ denotes the position error of the ith robot. The navigation control aims to minimize $\gamma(q_i(t))$. To achieve this goal, the control input is designed as a negative gradient of the potential function φ_i, that is,

$$u_i(t) = -k_i\frac{\partial\varphi_i}{\partial q_i(t)} \tag{10}$$

where k_i is a positive control gain.

Taking the derivative of φ_i with respect to $q_i(t)$ yields

$$\frac{\partial\varphi_i}{\partial q_i(t)} = \frac{G(q_i(t))\nabla\gamma(q_i(t)) - \frac{\gamma(q_i(t))}{\delta}\nabla G(q_i(t))}{\left(\gamma^\delta(q_i(t)) + G(q_i(t))\right)^{\frac{1}{\delta}+1}}. \tag{11}$$

Substituting (11) into (10), the control input becomes

$$u_i(t) = v_i\left(-e_i - \sum_{j\in N(i)}\pi_{ij}d_{ij} + \sum_{\ell(\varsigma)\in O(i)}\eta_{i\ell(\varsigma)}d_{i\ell(\varsigma)}\right) \tag{12}$$

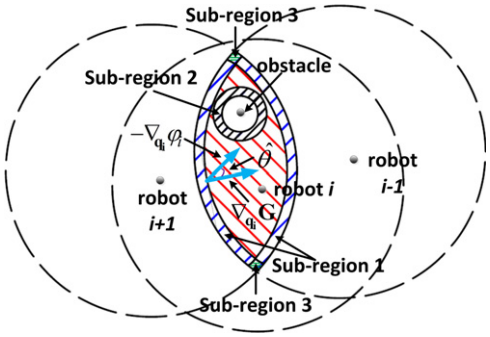

Fig. 3. Instance wherein the velocity of the ith robot agrees with the gradient of $G(q_i(t))$.

where $v_i = k_i G(q_i(t))\left(\gamma^{\delta}(q_i(t)) + G(q_i(t))\right)^{-\frac{1}{\delta}-1}$, $\pi_{ij} = \frac{\gamma(q_i(t))}{\delta\beta_{ij}}$, and $\eta_{i\ell(\varsigma)} = \frac{\gamma(q_i(t))}{\delta\alpha_{i\ell(\varsigma)}}$. The controller (12) includes three terms for navigation, connectivity, and obstacle avoidance, separately.

Substituting (12) into the robot dynamics in (1), the following closed-loop dynamics equation is obtained:

$$\dot{\mathbf{q}}(t) = (L_M \otimes I_2)\,\mathbf{q}(t) + (L_D \otimes I_2)\,\mathbf{q^d} + (L_O \otimes I_2)\,\mathbf{q_o} \tag{13}$$

where $\otimes$ denotes the Kronecker matrix product (Horn & Johnson, 1991); I_2 is a 2×2 identity matrix; L_D is an $n\times n$ real diagonal matrix with the diagonal element of $L_{Dii} = v_i$; and L_M is an $n\times n$ real matrix, whose diagonal elements are $L_{Mii} = v_i(-1 - \sum_{j\in N(i)}\pi_{ij} + \sum_{\ell(\varsigma)\in O(i)}\eta_{i\ell(\varsigma)})$. $L_{Mij} = v_i\pi_{ij}$ when $j\in N(i)$, and $L_{Mij} = 0$ when $j\notin N(i)$. Furthermore, L_O is an $n\times m$ matrix, with the element $L_{Oi\ell(\varsigma)} = -v_i\delta_{i\ell(\varsigma)}$ when $\ell(\varsigma)\in O(i)$, and $L_{Oi\ell(\varsigma)} = 0$ otherwise.

Theorem 1. *Consider n mobile robots with dynamics (1). Under the conditions that all the robots are located inside the free workspace at the initial configuration and $\mathbf{q^d}$ is reachable at the final configuration, the control law (12) gives rise to the following results:* (i) $G(q_i(t)) > 0, \forall t > 0$; (ii) *the underlying graph remains connected at all times; and* (iii) *the robots avoid all obstacles in the environment.*

Proof. We denote as $-\nabla_{q_i}\varphi_i$ the velocity of the ith robot, as $\nabla_{q_i}G(q_i(t))$ the gradient of $G(q_i(t))$, and as $\nabla_{q_i}(\cdot)$ the partial derivative of $(\cdot)$ with respect to $q_i(t)$. In the free workspace, substituting (10) into (12) and taking the inner product of $-\nabla_{q_i}\varphi_i$ and $\nabla_{q_i}G(q_i(t))$ yields

$$\begin{aligned}
&-\nabla_{q_i}\varphi\nabla G(q_i(t))\\
&= \frac{\nabla_{q_i}G(q_i(t))\left(\frac{\gamma(q_i(t))\nabla_{q_i}G(q_i(t))}{\delta} - G(q_i(t))\nabla_{q_i}\gamma(q_i(t))\right)}{\left(\gamma(q_i(t))^{\delta} + G(q_i(t))\right)^{\frac{1}{\delta}+1}}\\
&= \frac{\frac{\lambda^2}{2\delta} - G(q_i(t))\nabla_{q_i}\gamma(q_i(t))\nabla_{q_i}G(q_i(t))}{\left(\gamma(q_i(t))^{\delta} + G(q_i(t))\right)^{\frac{1}{\delta}+1}}\\
&\geq \frac{\lambda\left(\frac{\lambda}{2\delta} - G(q_i(t))\right)}{\left(\gamma(q_i(t))^{\delta} + G(q_i(t))\right)^{\frac{1}{\delta}+1}}
\end{aligned} \tag{14}$$

where $\lambda = \left\|\nabla_{q_i}\gamma(q_i(t))\right\|\left\|\nabla_{q_i}G(q_i(t))\right\|$.

A small neighborhood H_i near the boundary of the free workspace can be defined as follows:

$$\left\{ q_i(t) \,|\, 0 < \beta_{ij} < \frac{\xi}{2} \vee 0 < \alpha_{i\ell(\varsigma)} < \frac{\xi}{2},\ \forall j\in N(i), \ell(\varsigma)\in O(i) \right\} \tag{15}$$

where ξ denotes a small positive parameter. As shown in Fig. 3, H_i consists of sub-regions of three types relating to three different cases.

Case 1: When the ith robot locates inside the sub-region 1 in H_i formed by the robot $j\in N(i)$, the ith robot almost locates outside the communication range of the jth robot, and $0 < \beta_{ij} \leq \frac{\xi}{2}$.

Case 2: When the ith robot locates inside the sub-region 2 in H_i formed by the obstacle $\ell(\varsigma)\in O(i)$, the ith robot almost hits the obstacle $\ell(\varsigma)$, and $0 < \alpha_{i\ell(\varsigma)} \leq \frac{\xi}{2}$.

Case 3: When the ith robot locates inside the sub-region 3, which is an interaction region in H_i formed by more than one robot or obstacle in the set $N(i)\cup O(i)$, the ith robot almost locates outside the communication range of more than one robot or hits more than one obstacle.

It will be shown in the following that the ith robot will be located outside H_i and inside the free workspace under the proposed controller.

In case 1, we have $\lim_{\xi\to 0} G_c(q_i(t)) = 0$. Thus

$$\begin{aligned}
\nabla_{q_i}G(q_i(t)) &= \lim_{\xi\to 0}\left\| G_o(q_i(t))\nabla_{q_i}G_c(q_i(t))\right.\\
&\quad \left. + G_c(q_i(t))\nabla_{q_i}G_o(q_i(t))\right\|\\
&= \lim_{\xi\to 0}\left\| G_o(q_i(t))\nabla_{q_i}G_c(q_i(t))\right\|.
\end{aligned} \tag{16}$$

Substituting (3) into (16) yields

$$\begin{aligned}
&\nabla_{q_i}G(q_i(t))\\
&= \lim_{\xi\to 0}\left\| \sum_{l\in N(t), l\neq j}\overline{\beta}_{il}G_o(q_i(t))(q_i(t) - q_l(t))\right.\\
&\quad \left. + \overline{\beta}_{ij}G_o(q_i(t))\left(q_i(t) - q_j(t)\right)\right]\Big\|\\
&= G_o(q_i(t))\,\overline{\beta}_{ij}r
\end{aligned} \tag{17}$$

where $\overline{\beta}_{ij} = \prod_{\tau\in N(i),\tau\neq j}\beta_{i\tau}$, and $\lim_{\xi\to 0}\overline{\beta}_{il} = 0$. Substituting (17) into (14) yields

$$-\nabla_{q_i}\varphi_i\nabla_{q_i}G(q_i(t)) \geq \frac{2^{\delta}r^2\overline{\beta}_{ij}^2(G_o(q_i(t)))^2}{\delta(e_i)^{2\delta}} > 0. \tag{18}$$

Inequality (18) implies that when the ith robot is located almost outside the communication range of the jth robot, the velocity of the ith robot agrees with the gradient of $G(q_i(t))$ ($\hat{\theta} < \frac{\pi}{2}$) and converges toward the free workspace F_i (Fig. 3). Consequently, $\beta_{ij} \leq \frac{\xi}{2}$ never happens, and hence, $\beta_{ij} > \frac{\xi}{2}, \forall j\in N(i)$.

In case 2, a result similar to that of case 1 is obtained:

$$\begin{aligned}
-\nabla_{q_i}\varphi_i\nabla_{q_i}G(q_i(t)) &\geq \frac{2^{\delta}\overline{\alpha}_{i\varsigma}^2(\rho_o(\varsigma))^2(G_c(q_i(t)))^2}{\delta(e_i)^{2\delta}}\\
&> 0
\end{aligned} \tag{19}$$

where $\overline{\alpha}_{i\ell(\varsigma)} = \prod_{\ell(l)\in O(i),\ell(l)\neq\ell(\varsigma)}\alpha_{il}$. Inequality (19) implies that when the ith robot almost hits the obstacle $\ell(\varsigma)$, the velocity of the ith robot also agrees with the gradient of $G(q_i(t))$ and converges toward the free workspace F_i. Therefore, $\alpha_{i\ell(\varsigma)} \leq \frac{\xi}{2}$ never happens, and hence, $\alpha_{i\ell(\varsigma)} > \frac{\xi}{2}, \forall\ell(\varsigma)\in O(i)$.

In case 3, we have

$$G(q_i(t)) = 0, \quad \nabla_{q_i}G(q_i(t)) = 0. \tag{20}$$

Substituting (20) into (11) yields $-\nabla_{q_i}\varphi_i = 0$, which implies that $q_i(t)$ is a critical point of φ_i. Substituting (20) into (8) yields $\varphi_i = 1$, implying that φ_i achieves its maximum at the critical point $q_i(t)$. Because $G(q_i(t)) > 0$ at the initial configuration, no open set

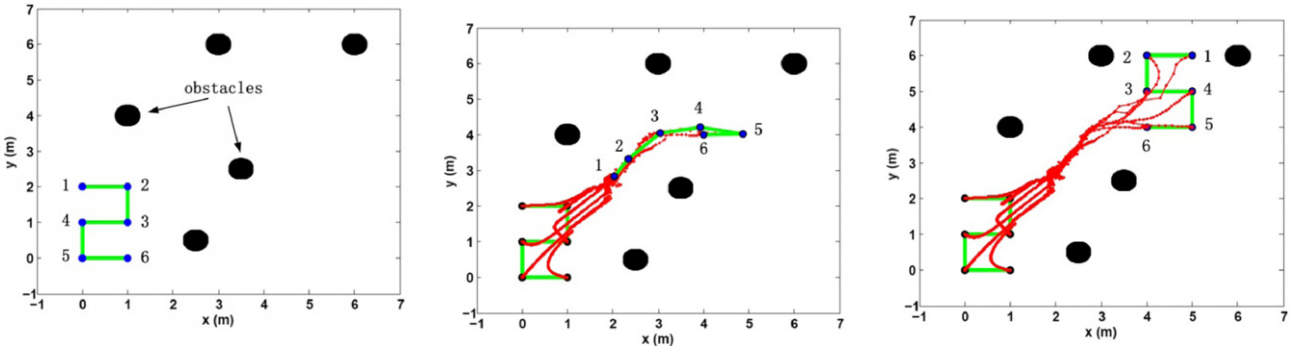

(a) 0 s. (b) 22 s. (c) 26 s.

Fig. 4. Switch from the initial configuration to the desired configuration.

of initial conditions can be attracted to the maximum of φ_i along its negative gradient (Dimarogonas & Johansson, 2008). Thus, case 3 never happens under controller (12).

Given a sufficiently small parameter ξ, Definition 2 suggests that the robots must locate outside H_i at the desired configuration. Therefore, both (18) and (19) hold at the desired configuration, implying that the ith robot is connected with all its neighbors under the conditions given in Theorem 1. Therefore, we conclude that $G(q_i(t)) > 0, \forall t > 0$, the underlying graph remains connected all the time, and the robots can avoid all obstacles in the environment. □

Theorem 2. *There exists a positive lower bound $\hat{\delta}$ on parameter δ (see (8)) such that the desired position q_i^d is the only critical point in the free workspace F_i, and q_i converges to q_i^d conditionally.*

Proof. q_i^d is clearly a non-degenerate minimum of φ_i, and the proof is omitted because of the limited space. We now discuss how to select δ such that q_i^d is the only critical point in the free workspace.

A function $\hat{\varphi}_i = \frac{\gamma(q_i(t))^\delta}{G(q_i(t))}$ is used instead of φ_i to analyze the polar property of φ_i (Rimon & Koditschek, 1992). q_c denotes a critical point of $\hat{\varphi}_i$. Taking the gradient of $\hat{\varphi}_i$ at $q_i(t) = q_c \neq q_i^d$, we have

$$\gamma(q_i(t))\nabla_{q_i}G(q_i(t)) = \delta G(q_i(t))\nabla_{q_i}\gamma(q_i(t)). \tag{21}$$

Expanding the term $\nabla_{q_i}G(q_i(t))$ with the triangle inequality yields

$$\delta \leq \frac{r^{2(m-|O(i)|)}\gamma(q_i(t))}{2^{m-|O(i)|}\left\|\nabla_{q_i}\gamma(q_i(t))\right\|} \times \left(\sum_{j\in N(i)}\frac{\|d_{ij}\|}{\beta_{ij}} + \sum_{\ell(\varsigma)\in O(i)}\frac{\|d_{i\ell(\varsigma)}\|}{\alpha_{i\ell(\varsigma)}}\right). \tag{22}$$

On the basis of $\frac{\|d_{ij}\|}{\beta_{ij}} \leq \frac{2r}{\xi}$ and $\frac{\|d_{i\ell(\varsigma)}\|}{\alpha_{i\ell(\varsigma)}} \leq \frac{2r}{\xi}$, it follows that

$$\delta \leq \frac{\|e_i\| r^{2(m-|O(i)|)+1}}{2^{m-|O(i)|}\xi}(|N(i)| + |O(i)|) \triangleq \hat{\delta}. \tag{23}$$

If inequality (23) does not hold, no critical point in the free workspace exists. Thus, a positive lower bound $\hat{\delta}$ exists, such as that for $\delta \geq \hat{\delta}$, and no other critical point exists in the free workspace. Isolated saddle points may exist in the free workspace, and the initial conditions that lead robots to saddle points are of zero measure, as stated in the study Rimon and Koditschek (1992). Therefore, the controller (12) can converge q_i to q_i^d conditionally. □

Note that the function φ_i is continuous and admissible, and the free workspace is compact. Thus, the navigation function-based controller (12) is naturally bounded (Rimon & Koditschek, 1992).

Table 1
Configurations of the robots and obstacles.

Position (m)	Index					
	1	2	3	4	5	6
$q_i(0)$	(0, 2)	(1, 2)	(1, 1)	(0, 1)	(0, 0)	(1, 0)
q_i^d	(5, 6)	(4, 6)	(4, 5)	(5, 5)	(5, 4)	(4, 4)
$q_o(\varsigma)$	(1, 4)	(3, 6)	(6, 6)	(3.5, 2.5)	(2.5, 0.5)	NA

Table 2
Control inputs of six robots.

Robot index	Maximum control inputs (m/s)	
	x-axis	y-axis
1	5.15	4.01
2	2.02	2.21
3	1.75	1.04
4	1.62	1.82
5	3.17	2.08
6	2.80	1.23

4. Simulation

Simulations were performed using a group of mobile robots to demonstrate the proposed approach. In a manner similar to that adopted by Ji and Egerstedt (2007) and Saber and Murray (2004), the second-smallest eigenvalue of the Laplacian matrix in the communication graph was used to demonstrate the connectivity performance.

In Fig. 4, the robots are denoted by points, and the communication links are denoted by the solid lines between two robots. Six robots with five communication links formed a shape of "2" in the initial state. The proposed controller was used to navigate a switch from shape "2" to shape "5" in the desired state. Obstacles are denoted by circles. The radii of the obstacles were set as $\rho_o(1) = \cdots \rho_o(5) = 0.3$ m. The configurations of robots and obstacles are listed in Table 1. The five communication links had the configurations of (1, 2), (2, 3), (3, 4), (4, 5), and (5, 6), respectively. The communication radius was set as $r = 1.4$ m. The parameter of the potential function was set as $\delta = 1.2$, and the feedback control gains were chosen as $k_1 = \cdots = k_6 = 10$. The sampling period was chosen as 10 ms in the simulations.

Fig. 4 illustrates the motion evolution under the controller (12). The curved lines denote the motion trajectories of the robots. No communication links were broken during the maneuver. For the purpose of comparison, Fig. 5 illustrates the robot motion evolution under the controller without connectivity maintenance (see, e.g., Rimon and Koditschek (1992)). The communication link (1, 2) was broken at 4 s.

Table 2 shows the maximum control inputs of the six robots under controller (12). The maximum velocities were below 5.15 m/s

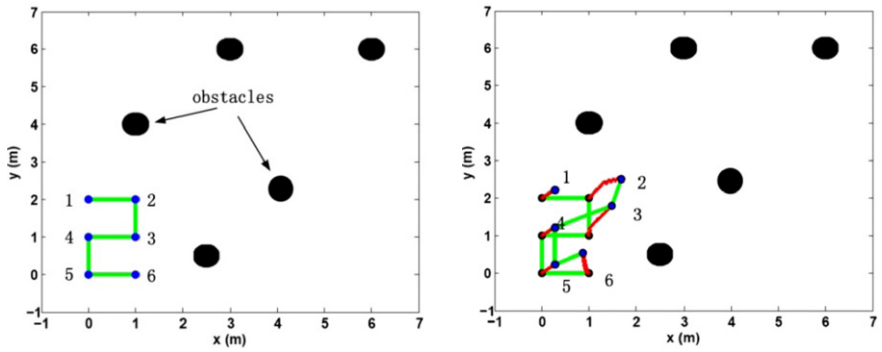

(a) 0 s. (b) 4 s.

Fig. 5. Example of connectivity failure in a navigation task.

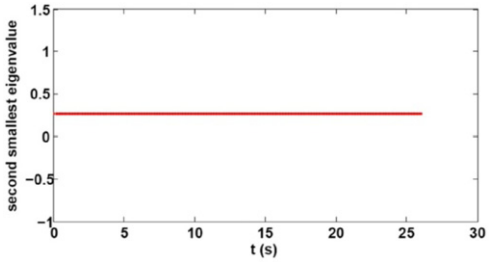

Fig. 6. Connectivity performance of networked robots.

in both the x and y directions, demonstrating that the proposed controller generated the bounded control inputs and could be feasibly realized in practice.

Fig. 6 illustrates the connectivity performance, where the second-smallest eigenvalue of the Laplacian matrix in the communication graph was always above zero.

This result implies that the communication graph remained connected during the navigation task. Fig. 7 illustrates the navigation performance of controller (12). All position errors of the six robots decreased to zero.

5. Experiment

Experiments were further performed on a group of four mobile robots to verify the proposed approach. The four robots were P3DX mobile robots denoted as robots 1–4. A P3DX robot employed control architecture with two levels, namely, one onboard PC for communication and programming and one 44.2368 MHz Renesas SH2 32-bit microprocessor for robot motion control. The robots communicated with one another via a 54.0 MHz wireless access point. Upon receiving the posture information of the robot, PC-104 generated the velocity input on the basis of the proposed controller and then sent the signal to the LM296 motor control unit. Each robot was equipped with a sonar system to detect obstacles. The robot motion state was measured using a motor encoder.

Table 3
Configurations of the robots and obstacles.

Position (m)	Index			
	1	2	3	4
$q_i(0)$	(1.2, 0)	(0, 1.2)	(−1.2, 0)	(0, −1.2)
q_i^d	(0, 1.2)	(−1.2, 0)	(0, −1.2)	(1.2, 0)
q_o (ς)	(0.72, 0.6)	(−0.72, 0.36)	NA	NA

Table 4
Control inputs of four robots.

Robot index	Maximum control inputs (m/s)	
	x-axis	y-axis
1	0.103	0.081
2	0.140	0.183
3	0.266	0.120
4	0.121	0.203

The four robots were controlled to accomplish a formation switching task in the presence of obstacles. The configuration of robots and obstacles is listed in Table 3. The parameter of the potential function was set as $\delta = 2.2$. The feedback control gains were $k_1 = \cdots = k_4 = 0.5$. The radius of the communication circle was $r = 2.1$ m. The physical radius of each P3DX robot is $r_R = 0.25$ m. The sampling time period was 100 ms.

Fig. 8 illustrates the formation switching process recorded through a video. The two long lines denote the x and y coordinate axes. The dotted arrows denote the motion directions of the robots. The desired formation switching task in the presence of obstacles was completed successfully.

Table 4 lists the maximum control inputs of the four robots under controller (12), and all of them were not high and could

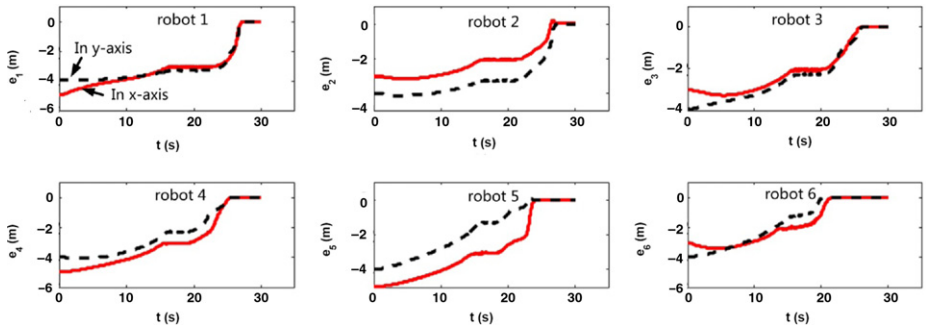

Fig. 7. Position errors of the six robots.

(a) Beginning. (b) 7 s. (c) 26 s.

Fig. 8. Evolution of the formation switching task using four robots: (a) initial robot configuration, (b) robot configuration after 7 s, and (c) completion of formation switching task after 26 s.

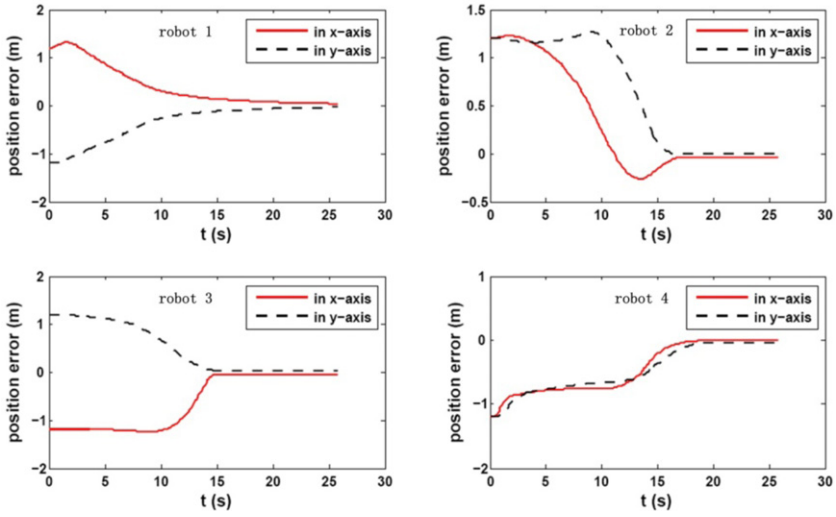

Fig. 9. Position errors of the four robots.

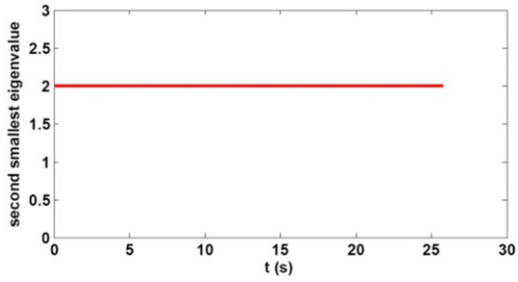

Fig. 10. Connectivity performance.

be easily realized. Fig. 9 illustrates the navigation performance of the four robots. All position errors of the four robots converged to zero. Fig. 10 illustrates the second-smallest eigenvalue of the communication graph during the maneuver, which was always larger than zero, implying that the underlying graph remained connected during the motion. These results demonstrate that controller (12) could achieve both connectivity and navigation successfully in the current experiment.

6. Conclusion

This paper presents a control approach to solving the multi-robot navigation problem while maintaining robot connectivity with bounded control inputs in the presence of obstacles. Compared with the existing approaches, the proposed method employs a new concept of connectivity constraint in building the objective function and a continuous model in formulating the obstacle avoidance. The proposed navigation function-based controller can achieve network connectivity, obstacle avoidance, and multirobot navigation simultaneously. In addition, the proposed controller generates a bounded control input, making it more feasible for practical applications. Both simulations and experiments were performed to demonstrate the effectiveness of the proposed approach. Future work will consider the dynamic communication topology in the control design.

References

Ando, H., Oasa, Y., Suzuki, I., & Yamashita, M. (1999). Distributed memoryless point convergence algorithm for mobile robots with limited visibility. *IEEE Transactions on Robotics and Automation*, *15*(5), 818–828.

Ayanian, N., & Kumar, V. (2008). Decentralized feedback controllers for multi-agent teams in environments with obstacles. In *IEEE international conference on robotics and automation* (pp. 1936–1941).

Cheah, C. C., Hou, S. P., & Slotine, J. J. E. (2009). Region-based shape control for a swarm of robots. *Automatica*, *45*(10), 2406–2411.

Cheah, C. C., Wang, D. Q., & Sun, Y. C. (2007). Region-reaching control of robots. *IEEE Transactions on Robotics*, *23*(6), 1260–1264.

Chen, H., Sun, D., Yang, J., & Chen, J. (2010a). Localization for multi-robot formations in indoor environment. *IEEE/ASME Transactions on Mechatronics*, *15*(4), 561–574.

Chen, J., Sun, D., Yang, J., & Chen, H. (2010b). A leader–follower formation control of multiple nonholonomic mobile robots incorporating receding-horizon scheme. *The International Journal of Robotics Research*, *29*(6), 727–747.

Cortes, J., Martinez, S., Karatas, T., & Bullo, F. (2004). Coverage control for mobile sensing networks. *IEEE Transactions on Robotics and Automation*, *20*(2), 243–255.

Cortes, J., Martinez, S., Karatas, T., & Bullo, F. (2005). Spatially-distributed coverage optimization and control with limited-range interactions. *ESAIM: Control Optimisation and Calculus of Variations*, *11*, 691–719.

DeGennaro, M.C., & Jadbabaie, A. (2006). Decentralized control of connectivity for multi-agent system. In *Proceedings of IEEE conference on decision and control* (pp. 3628–3633).

Dimarogonas, D.V., & Johansson, K.H. (2008). Decentralized connectivity maintains in mobile networks with bounded inputs. In *Proceedings of IEEE international conference on robotics and automation* (pp. 1507–1512).

Gazi, V., & Passino, K. M. (2004). A Class of attractions/repulsion functions for stable swarm aggregations. *International Journal of Control*, *77*(18), 1567–1579.

Guo, Y., & Balakrishnan, M. (2006). Complete coverage control for nonholonomic mobile robots in dynamic environment. In *Proceedings of IEEE international conference on robotics and automation* (pp. 1704–1709).
Guo, Y., & Qu, Z. (2008). Control of frictional dynamics of a one-dimensional particle array. *Automatica*, *44*(10), 2560–2569.
Horn, R. A., & Johnson, C. R. (1991). *Topics in matrix analysis*. Cambridge University Press.
Ji, M., & Egerstedt, M. (2007). Distributed coordination control of multiagent systems while preserving connectedness. *IEEE Transactions on Robotics*, *43*(4), 693–703.
Kim, Y., & Mesbahi, M. (2005). On maximizing the second smallest eigenvalue of a state dependent graph laplacian. In *Proceedings of American control conference* (pp. 99–103).
Li, X., Sun, D., & Yang, J. (2010). Multirobot consensus while preserving connectivity in presence of obstacles with bounded control inputs. In *Proceedings of IEEE/RSJ international conference on intelligent robots and systems*. Taiwan. Oct. 15–17.
Li, X., Sun, D., Yang, J., & Liu, S. (2011). Connectivity constrained multirobot navigation while considering physical size of robots. In *The 5th IEEE international conference on automation and logistics* (pp. 24–29).
Liu, S., Sun, D., & Zhu, C. (2011). Coordinated motion planning for multiple mobile robots along designed paths with formation requirement. *IEEE/ASME Transactions on Mechatronics*, *16*(6), 1021–1031.
Loizou, S. G., & Kyriakopoulos, K. J. (2006). A feedback-based multiagent navigation framework. *International Journal of System Science*, *37*(6), 377–384.
Lu, Y., & Guo, Y. (2010). Multi-agent flocking with formation in a constrained environment. *Journal of Control Theory and Applications*, *8*(2), 151–159.
Lumelsky, J., & Harinarayan, K. R. (1997). Decentralized motion planning for multiple mobile robots: the cocktail party model. *Autonomous Robots*, *4*(1), 121–136.
Ren, W., & Beard, R. W. (2005). Consensus seeking in multiagent systems under dynamically changing interaction topologies. *IEEE Transactions on Automatic Control*, *50*(5), 655–661.
Rimon, E., & Koditschek, D. E. (1992). Exact robot navigation using artificial potential functions. *IEEE Transactions on Robotics and Automation*, *8*(5), 501–518.
Saber, R. O. (2006). Flocking with multi-agent dynamic systems: algorithms and theory. *IEEE Transactions on Automatic Control*, *51*(3), 401–420.
Saber, R. O., & Murray, R. M. (2004). Consensus problem in networks of agents with switch topology and time-delay. *IEEE Transactions on Automatic Control*, *49*(9), 1520–1533.
Savla, K., Notarstefano, G., & Bullo, F. (2009). Maintaining limited-range connectivity among second-order agents. *SIAM Journal on Control and Optimization*, *15*(5), 187–205.
Sheng, W., Yang, Q., Tan, J., & Xi, N. (2006). Distributed multi-robot coordination in area exploration. *Robotics and Autonomous System*, *54*, 945–955.
Shi, H., Wang, L., & Chu, T.G. (2006). Coordinated control of multiple interactive dynamic agents with asymmetric coupling pattern and switching topology. In *Proceedings of IEEE/RSJ international conference on intelligent robots and systems* (pp. 3209–3214).
Spanos, D.P., & Murray, R.M. (2004). Robust connectivity of networked vehicles. In *Proceedings of IEEE conference on decision and control* (pp. 2893–2898).
Stipanović, D. M., Hokayem, P. F., Spong, M. W., & Šiljak, D. D. (2007). Avoidance control for multi-agent systems. *ASME Journal of Dynamic Systems, Measurement, and Control*, *29*, 699–707.
Stump, E., Jadbabaie, A., & Kumar, V. (2008). Connectivity management in mobile robot teams. In *Proceedings of IEEE international conference on robotics and automation* (pp. 1525–1530).
Sun, D., Wang, C., Shang, W., & Feng, G. (2009). Synchronization approach to trajectory tracking of multiple mobile robots while maintaining time-varying formations. *IEEE Transactions on Robotics*, *25*(5), 1074–1086.
Tanner, H., Jadbabaie, A., & Pappas, G. J. (2007). Flocking in fixed and switching networks. *IEEE Transactions on Automatic Control*, *52*(5), 863–868.
Tardioli, D., Mosteo, A. R., Riazuelo, L., Villarroel, J. L., & Montano, L. (2010). Enforcing network connectivity in robot team missions. *International Journal of Robotics Research*, *29*(4), 460–480.
Tekdas, O., Kumar, Y., Isler, V., & Janardan, R. (2012). Building a communication bridge with mobile Hubs. *IEEE Transactions on Automation Science and Engineering*, *9*(1), 171–176.
Wang, H., & Guo, Y. (2008). Consensus on scale-free networks. In *Proceedings of American control conference* (pp. 748–752).
Yan, X., Chen, J., & Sun, D. (2012). Multilevel-based topology design and shape control of robot swarms. *Automatica*, *48*(12), 3122–3127.
Zavlanos, M. M., Tanner, H. G., Jadbabaie, A., & Pappas, G. J. (2009). Hybrid control for connectivity preserving flocking. *IEEE Transactions on Automatic Control*, *54*(12), 2869–2875.
Zheng, Y., & Chen, W. (2007). Mobile robot team forming for crystallization of proteins. *Autonomous Robots*, *23*(1), 69–78.

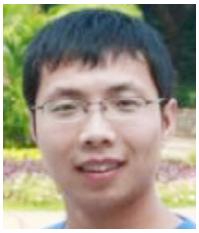

Xiangpeng Li received the B.Sc. in mechatronics and automation from Harbin Institute of Technology, Harbin, China, and Ph.D. degrees in robotics and automation from both the University of Science and Technology of China and City University of Hong Kong, Kowloon, Hong Kong. He is currently a post-doctoral researcher in CityU–USTC joint advanced research center, Suzhou, China. His research interests include robot networks and robot-assisted biomedical systems.

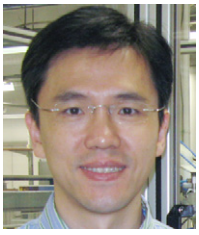

Dong Sun received the Bachelor and Master's degrees in mechatronics and biomedical engineering from Tsinghua University, Beijing, China, and the Ph.D. degree in robotics and automation from the Chinese University of Hong Kong, Hong Kong. He was a post-doctoral researcher at the University of Toronto, Toronto, ON, Canada, and a research and development engineer in industry in Ontario. Since 2000, he has been with the City University of Hong Kong, Kowloon, Hong Kong, where he is now a professor in the Department of Mechanical and Biomedical Engineering. His research interests include robotics manipulation, multirobot systems, motion control, and cell-based bioengineering. Prof. Sun was an Associate Editor for the IEEE Transactions on Robotics from 2004 to 2008. He currently serves as a Technical Editor for the IEEE/ASME Transactions on Mechatronics.

Jie Yang received the B.Sc. degree in the physics of metals from the University of Science and Technology of Beijing, Beijing, China, in 1969. He is now a professor in the Department of Precision Machinery and Precision Instrumentations at the University of Science and Technology of China. His current research interests include robotics and mechatronics.